Supplement of Atmos. Meas. Tech., 16, 3039–3057, 2023
https://doi.org/10.5194/amt-16-3039-2023-supplement

Atmospheric Measurement Techniques
Open Access
EGU

Supplement of

Satellite-based, top-down approach for the adjustment of aerosol precursor emissions over East Asia: the TROPOspheric Monitoring Instrument (TROPOMI) NO_2 product and the Geostationary Environment Monitoring Spectrometer (GEMS) aerosol optical depth (AOD) data fusion product and its proxy

Jincheol Park et al.

Correspondence to: Yunsoo Choi (ychoi6@uh.edu)

Table S1. Model configurations.

WRF 3.8	
Domain	East Asia on 27 km × 27 km grids
Microphysics	Morrison's double-moment scheme (Morrison *et al*., 2009)
Longwave and shortwave radiation	Rapid Radiative Transfer Model for GCMs (RRTMG) (Clough *et al*., 2005; Iacono *et al*., 2008)
Land surface	Pleim-Xiu land surface model (Xiu and Pleim, 2001)
Surface layer	Pleim-Xiu surface layer (Pleim, 2006)
Planetary boundary layer	ACM2 planetary boundary layer model (Pleim 2007a, 2007b)
Cumulus parameterization	Kain-Fritch (new Eta) scheme (Kain, 2004)
Four-Dimensional Data Assimilation	FDDA option for grid-nudging (Jeon *et al*., 2015)
Initial and boundary conditions for meteorology	1° × 1° National Centers for Environmental Prediction (NCEP) FNL (final) operational model global analysis data
CMAQ 5.2 and CMAQ DDM-3D 5.2	
Horizontal advection	YAMO
Vertical advection	WRF omega formula
Horizontal diffusion	Multiscale
Vertical diffusion	ACM2 vertical diffusion scheme (Pleim 2007a, 2007b)
Chemical mechanism and aerosol processing module	SAPRC-07 and AERO6 (Carter, 2010; Simon, 2015)
Dry deposition model	M3Dry (Pleim *et al*., 2001)

Table S2. The list of the primary PM species included the KORUS-AQ emission inventory and the corresponding pollutants simulated in CMAQ version 5.2 and measured at the Korean supersites. Note that all emissions species listed are primary, and some corresponding species include both primary and secondary forms of themselves.

KORUS-AQ emissions species	Corresponding CMAQ species	Corresponding Korean supersite species	Description
PSO4	ASO4J	$PM_{2.5}SO_4$	Fine mode sulfate
PNO3	ANO3J	$PM_{2.5}NO_3$	Fine mode nitrate
PCL	ACLJ	$PM_{2.5}Cl$	Fine mode particulate chloride
PNH4	ANH4J	$PM_{2.5}NH_4$	Fine particulate ammonium
PNA	ANAJ	$PM_{2.5}Na$	Fine mode sodium
PCA	ACAJ	$PM_{2.5}Ca$	Fine mode calcium
PMG	AMGJ	$PM_{2.5}Mg$	Fine mode magnesium
PK	AKJ	$PM_{2.5}K$	Fine mode potassium
POC	APOCI, APOCJ	$PM_{2.5}OC$	Fine mode primary organic carbon
PNCOM	APNCOMI, APNCOMJ	-	Fine mode primary non-carbon organic matter
PEC	AECI, AECJ	$PM_{2.5}EC$	Fine mode elemental carbon
PFE	AFEJ	$PM_{2.5}Fe$	Fine mode iron
PAL	AALJ	-	Fine mode aluminum
PSI	ASIJ	-	Fine mode silicon
PTI	ATIJ	$PM_{2.5}Ti$	Fine mode titanium
PMN	AMNJ	$PM_{2.5}Mn$	Fine mode manganese
PH2O	AH2OJ	-	Fine mode particulate water
PMOTHR	AOTHRJ	$PM_{2.5}V$, $PM_{2.5}Cr$, $PM_{2.5}Ni$, $PM_{2.5}Cu$, $PM_{2.5}Zn$, $PM_{2.5}As$, $PM_{2.5}Se$, $PM_{2.5}Br$, $PM_{2.5}Pb$	Remaining unspeciated (undefined) fine mode primary PM
PMC	ACORS	-	Coarse mode primary PM

Table S3. Summary statistics between the WRF-simulated hourly meteorological fields (2 m air temperatures (°C), and 10 m wind U and V components (m/s)) and ground-based in-situ measurements in Korea during the study periods 2019 (132 sites) and 2022 (95 sites). R: Pearson's correlation coefficient, IOA: index of agreement, RMSE: root mean square error, MB: mean bias.

	2019			2022		
	Air temperature	Wind U	Wind V	Air temperature	Wind U	Wind V
R	0.98	0.64	0.52	0.95	0.65	0.48
IOA	0.99	0.74	0.69	0.96	0.75	0.66
RMSE	2.34	1.68	1.55	2.81	1.56	1.41
MB	-1.00	0.16	-0.21	-1.56	0.49	0.02

Table S4. Seasonal and yearly mean NO_x emissions (tons/day) before (a priori) and after (a posteriori) the NO_x emissions adjustment over the modeling domain during the study period 2019. MAM: March, April, and May, JJA: June, July, and August, SON: September, October, and November, DJF: December, January, and February.

	MAM	JJA	SON	DJF	Yearly
A priori	2.21	2.28	2.17	2.17	2.21
A posteriori	4.98	6.25	4.72	3.73	4.92
Difference (post - prior) (%)	125.08	174.16	117.68	71.64	122.79

Table S5. Summary statistics of the CMAQ-simulated daily mean surface NO_2 concentrations (ppb) before (a priori) and after (a posteriori) the NO_x emission adjustment and ground-based in-situ measurements (346 sites in Korea and 235 sites in the NCP region) during the study period 2019. R: Pearson's correlation coefficient; NMB (%): normalized mean bias.

		Korea		NCP	
		A priori	A posteriori	A priori	A posteriori
MAM	R	0.66	0.72	0.75	0.75
	NMB	-24.20	-5.66	-13.90	12.34
JJA	R	0.45	0.63	0.54	0.52
	NMB	15.63	1.83	5.25	22.32
SON	R	0.72	0.82	0.50	0.55
	NMB	-2.06	21.66	-11.43	15.24
DJF	R	0.75	0.76	0.55	0.59
	NMB	-23.54	13.45	-1.05	33.75
Yearly	R	0.71	0.84	0.76	0.78

	NMB	-12.11	8.51	-6.00	21.70

Table S6. Seasonal and yearly mean primary PM emissions (g/s) before (a priori) and after (a posteriori) the primary PM emissions adjustments (the emissions adjustments using the AHI AOD and GOCI-AHI fused AOD) over the modeling domain during the study period 2019. The primary PM emissions here indicate the total amount of all primary PM species listed in Table S2.

		MAM	JJA	SON	DJF	Yearly
Emissions adjusted using AHI AOD	A priori	13.45	11.90	12.35	15.19	13.22
	A posteriori	21.19	21.61	19.55	31.79	23.53
	Difference (post - prior) (%)	57.54	81.62	58.27	109.30	76.68
Emissions adjusted using GOCI-AHI AOD	A priori	13.45	11.90	12.35	15.19	13.22
	A posteriori	28.28	28.91	23.16	33.08	28.36
	Difference (post - prior) (%)	110.30	142.96	87.54	117.73	114.63

Table S7. Monthly and 3-month mean NO_x emissions (tons/day) before (a priori) and after (a posteriori) the NO_x emissions adjustment over the modeling domain during the study period 2022.

	MAR	APR	MAY	3-month
A priori	0.83	0.82	0.82	0.82
A posteriori	0.80	0.71	0.76	0.76
Difference (post - prior) (%)	-2.83	-13.40	-7.33	-7.84

Table S8. Monthly and 3-month mean primary PM emissions (g/s) before (a priori) and after (a posteriori) the primary PM emissions adjustments (using GEMS-AMI-GOCI-2 fused AOD) over the modeling domain during the study period 2022. The primary PM emissions here indicate the total amount of all primary PM species listed in Table S2.

	MAR	APR	MAY	3-month
A priori	14.61	12.80	12.61	13.34
A posteriori	10.35	13.67	12.38	12.14
Difference (post - prior) (%)	-29.17	6.86	-1.81	-9.03

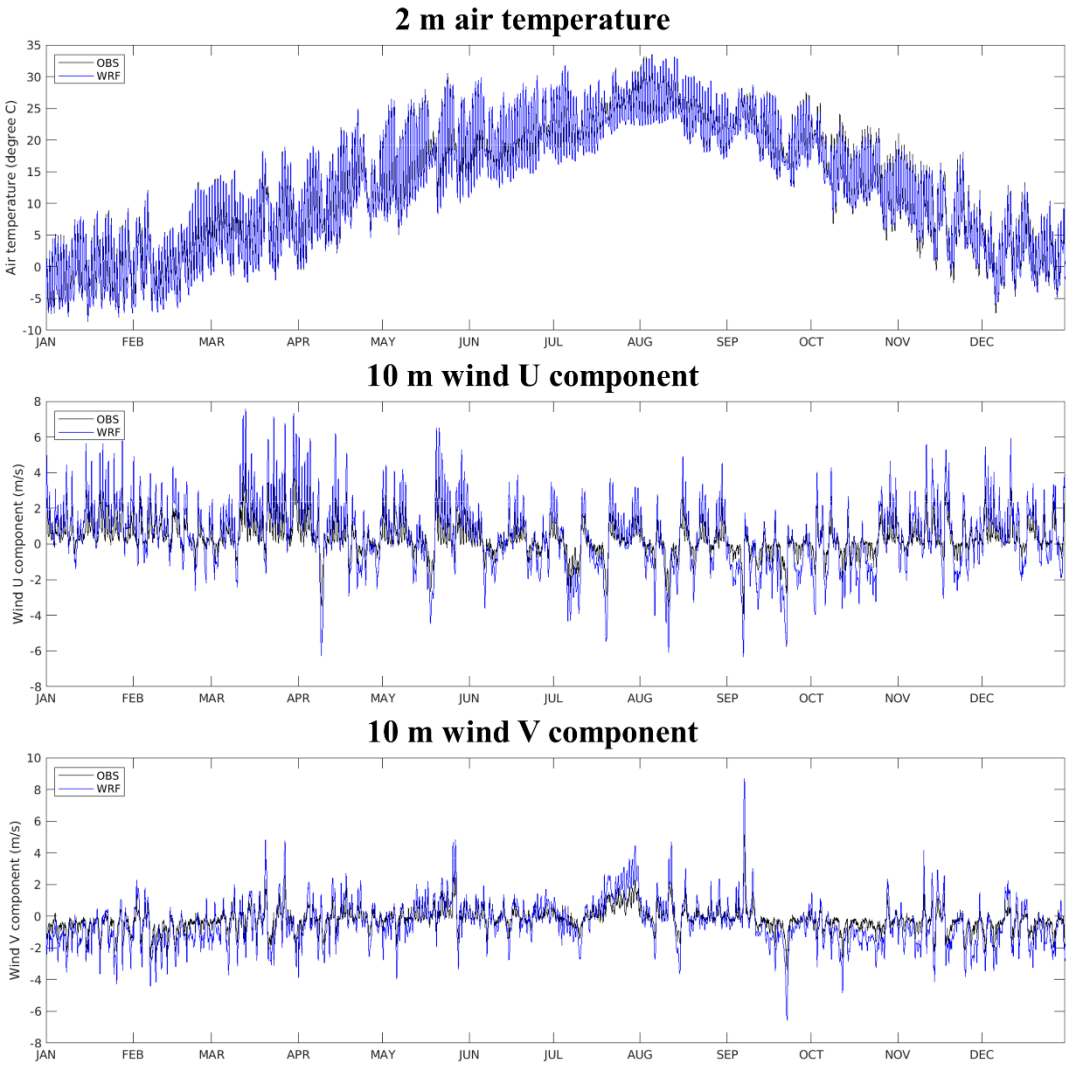

Figure S1. Time-series comparisons between WRF-simulated hourly meteorological fields (2 m air temperatures (°C) and 10 m wind U and V components (m/s)) and ground-based in-situ measurements in Korea during the study period 2019 (132 sites). OBS: ground-based in-situ measurements, WRF: WRF-simulated meteorological fields.

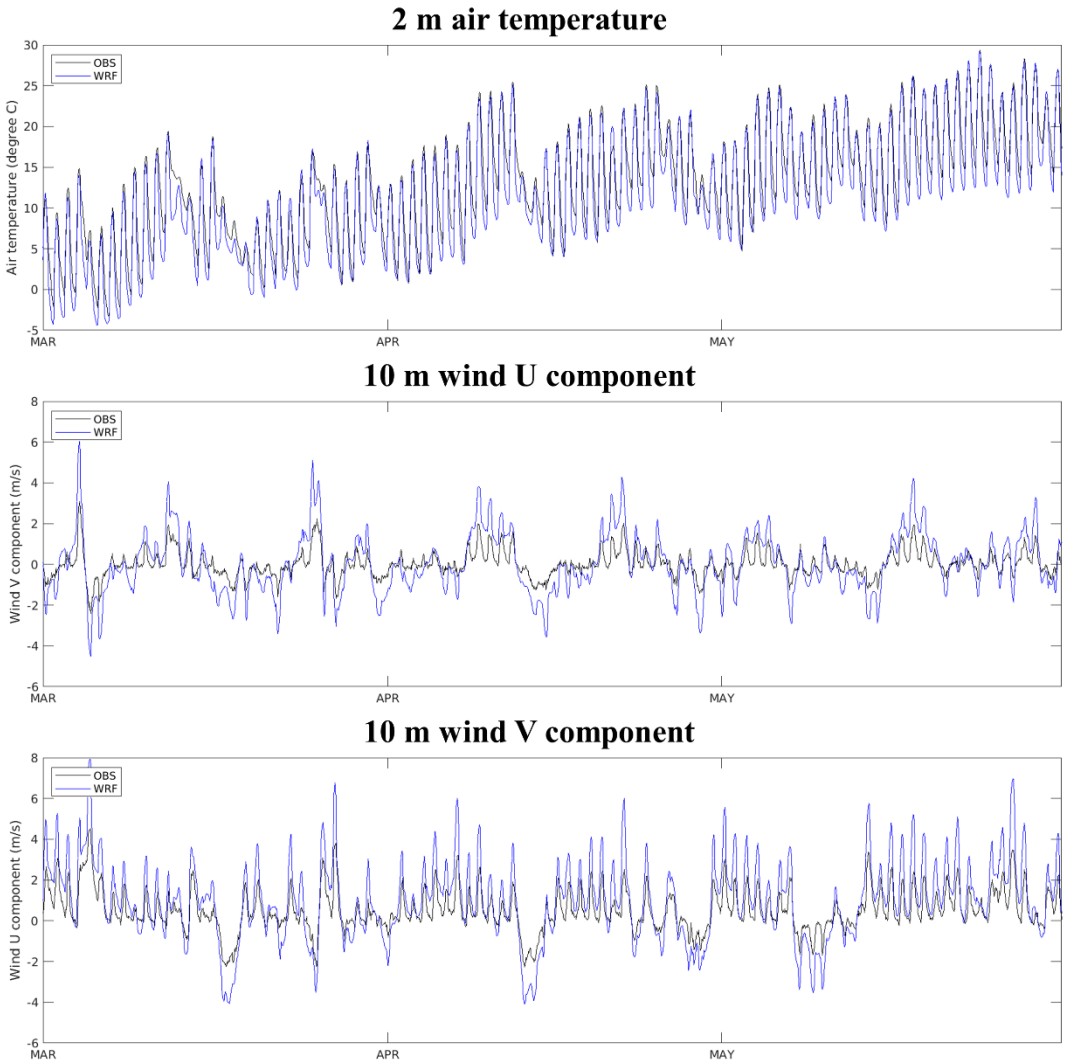

40 **Figure S2. Time-series comparisons between WRF-simulated hourly meteorological fields (2 m air temperatures (°C) and 10 m wind U and V components (m/s)) and ground-based in-situ measurements in Korea during the study period 2022 (95 sites). OBS: ground-based in-situ measurements, WRF: WRF-simulated meteorological fields.**

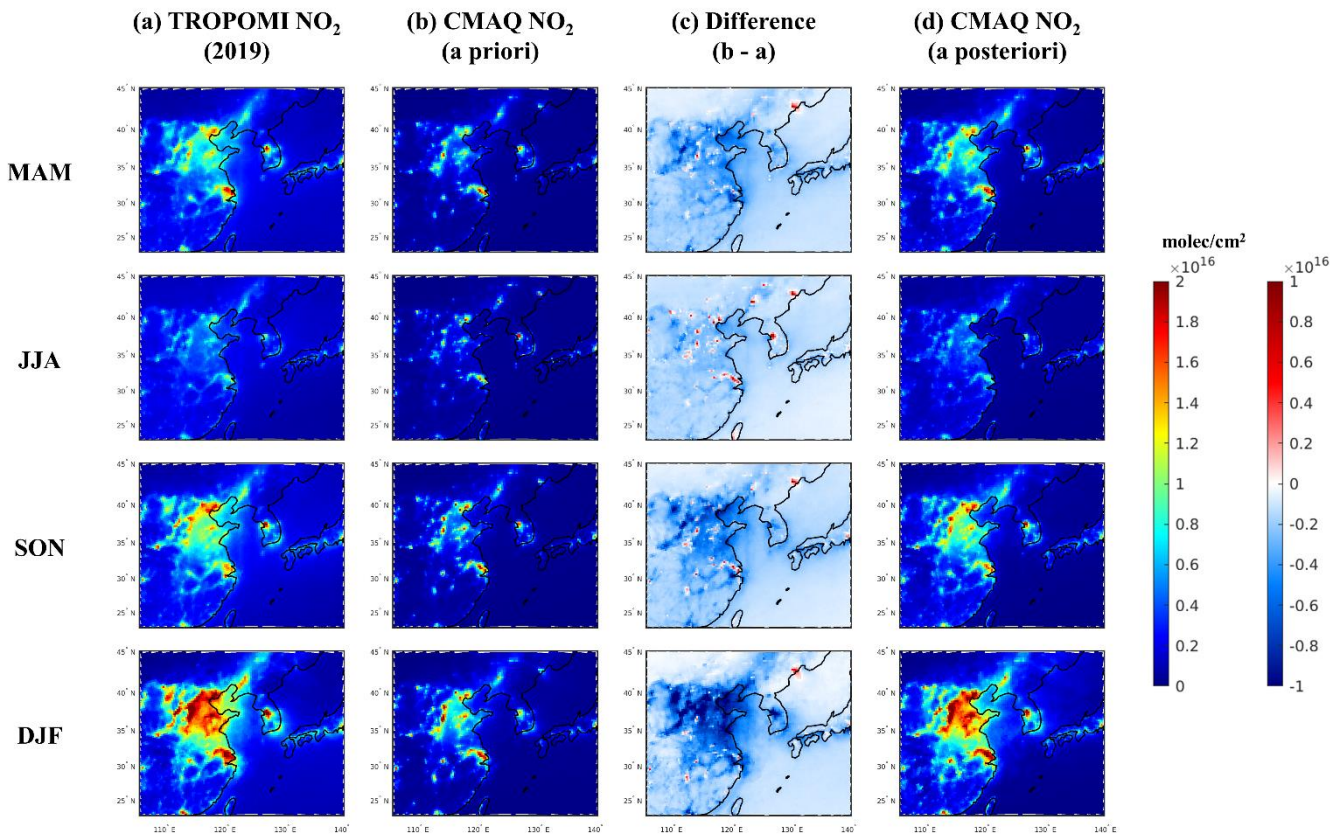

45 **Figure S3. Spatial distributions of (a) TROPOMI NO_2 columns (molec/cm^2) and CMAQ-simulated NO_2 columns (b) before and (d) after the NO_x emissions adjustment during the study period 2019. MAM: March, April, and May; JJA: June, July, and August; SON: September, October, and November; DJF: December, January, and February.**

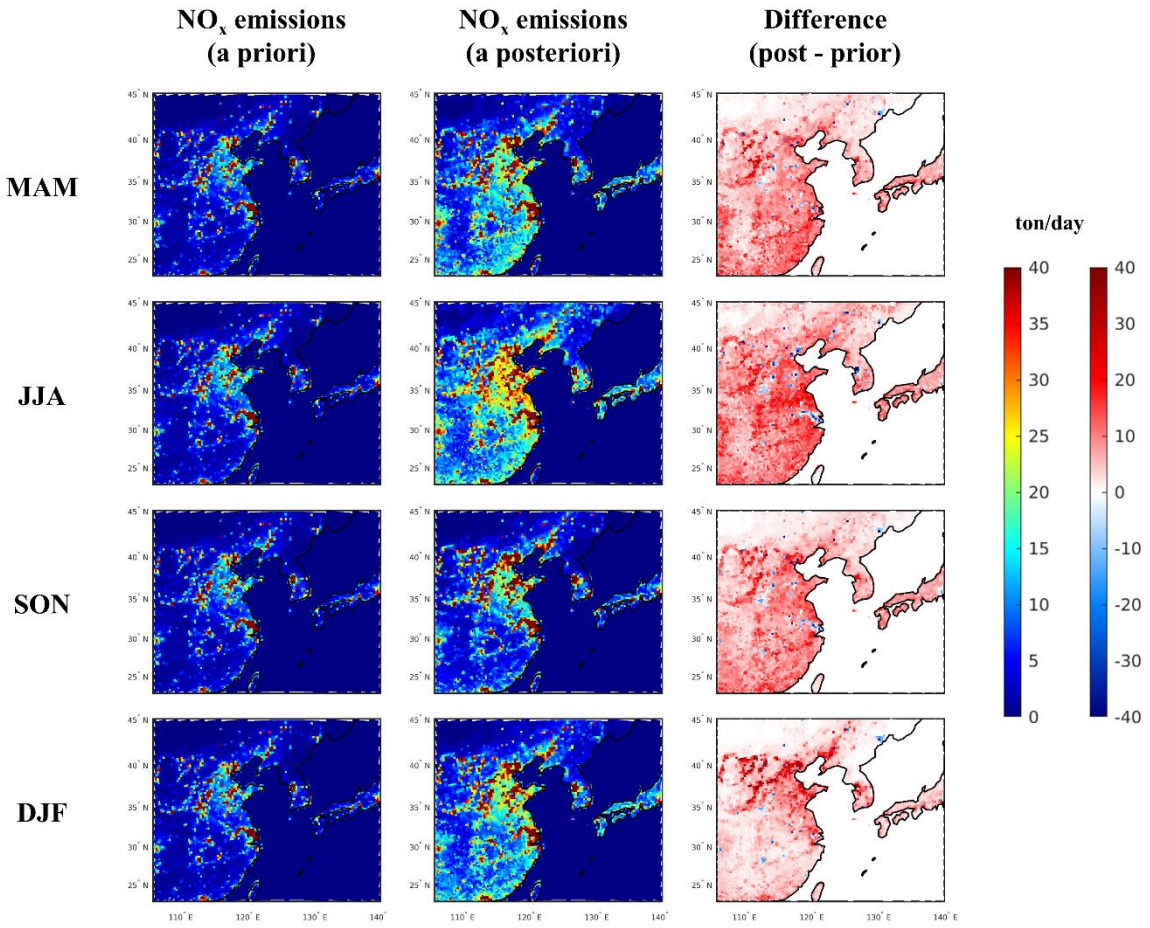

Figure S4. Spatial distributions of the bottom-up estimates of NO_x emissions (ton/day) before (a priori) and after (a posteriori) the NO_x emissions adjustment during the study period 2019.

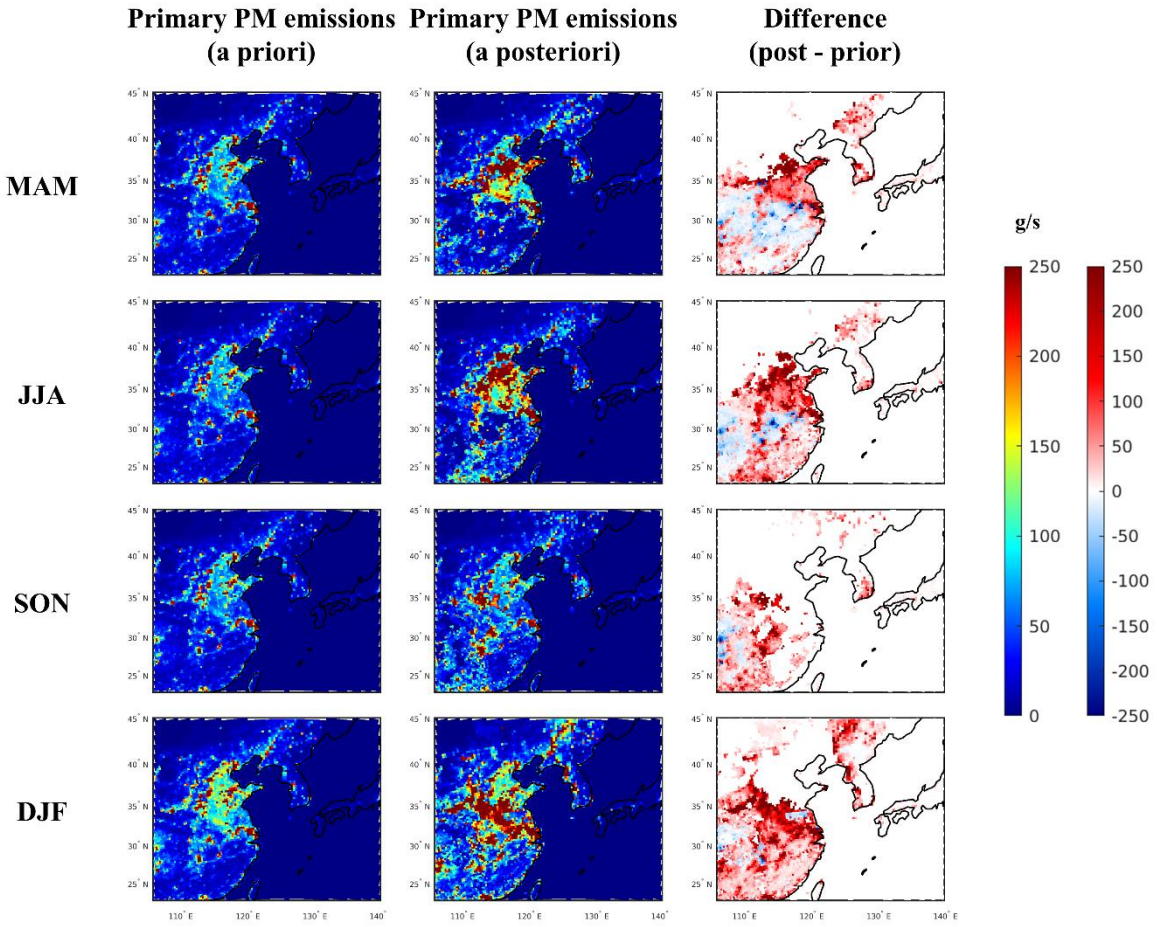

Figure S5. Spatial distributions of TROPOMI NO_2 columns and CMAQ-simulated NO_2 columns before (a priori) and after (a posteriori) the NO_x emissions adjustment during the study period 2019. MAM: March, April, and May; JJA: June, July, and August; SON: September, October, and November; and DJF: December, January, and February.

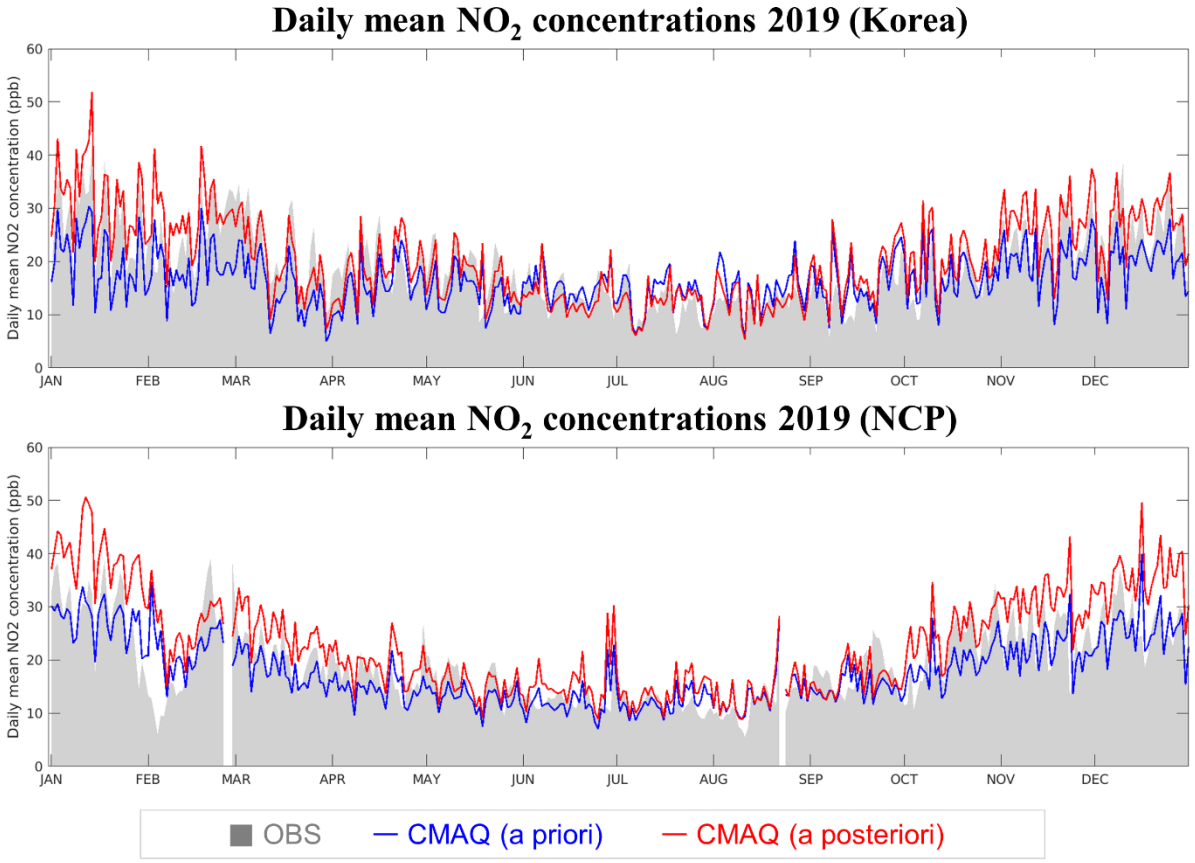

Figure S6. Comparisons of the time-series of the CMAQ-simulated daily mean surface NO_2 concentrations (ppb) before (a priori) and after (a posteriori) the NO_x emission adjustment and the ground-based in-situ measurements in Korea (346 AirKorea sites) and the NCP region (235 MEE sites) during the study period 2019. OBS: ground-based in-situ measurements.

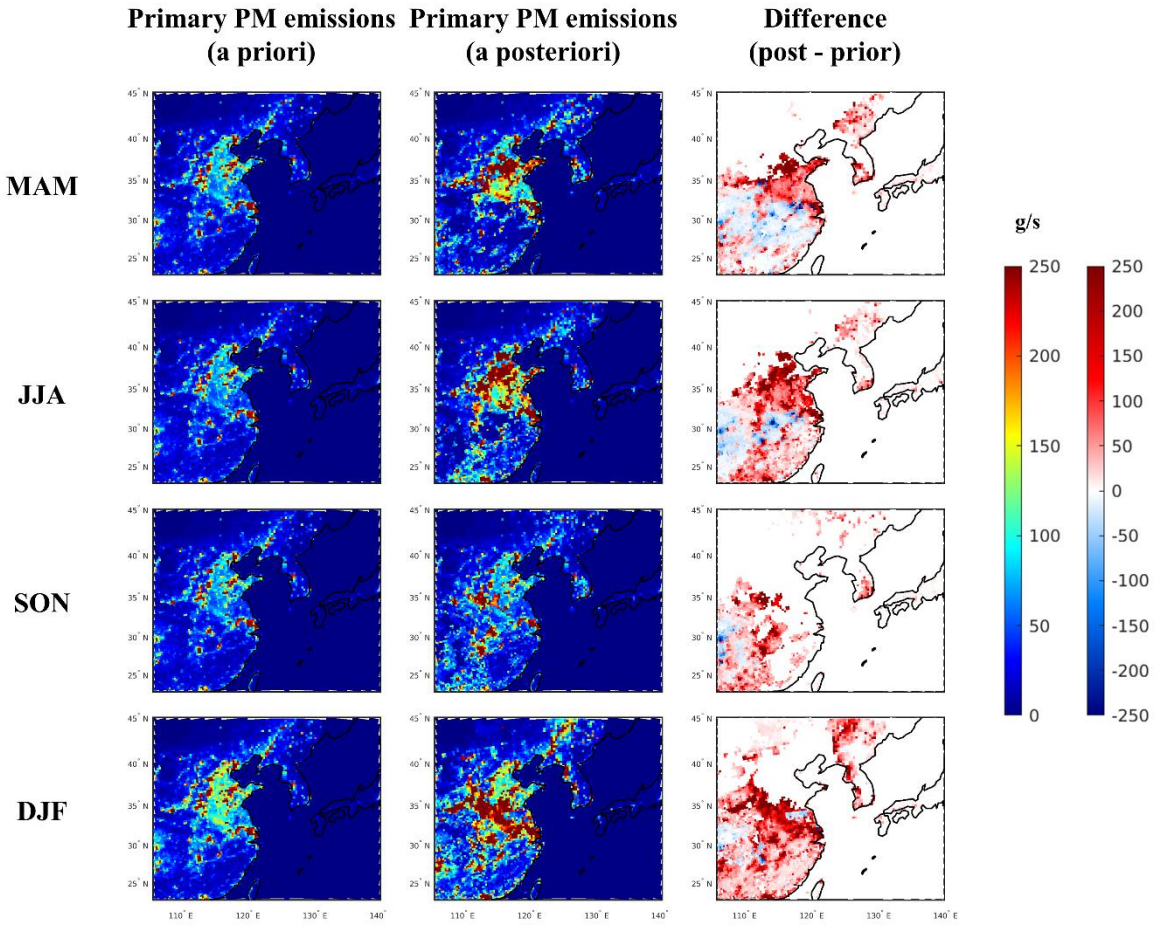

Figure S7. Spatial distributions of the bottom-up estimates of primary PM emissions (g/s) before (a priori) and after (a posteriori) the primary PM emissions adjustment (using the AHI AOD) during the study period 2019. The primary PM emissions here indicate the total amount of all primary PM species listed in Table S2.

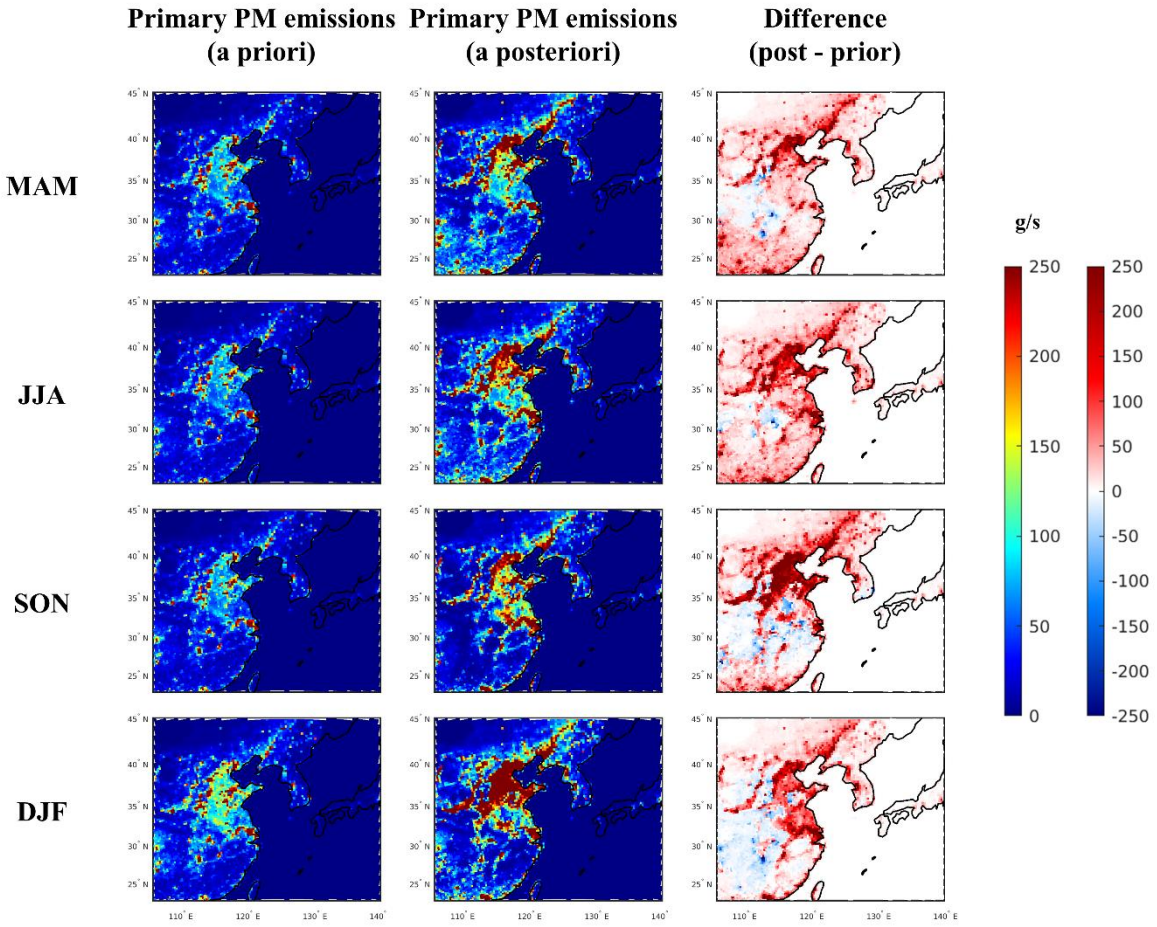

Figure S8. Spatial distributions of the bottom-up estimates of primary PM emissions (g/s) before (a priori) and after (a posteriori) the primary PM emissions adjustment (using GOCI-AHI fused AOD) during the study period 2019. The primary PM emissions here indicate the total amount of all primary PM species listed in Table S2.

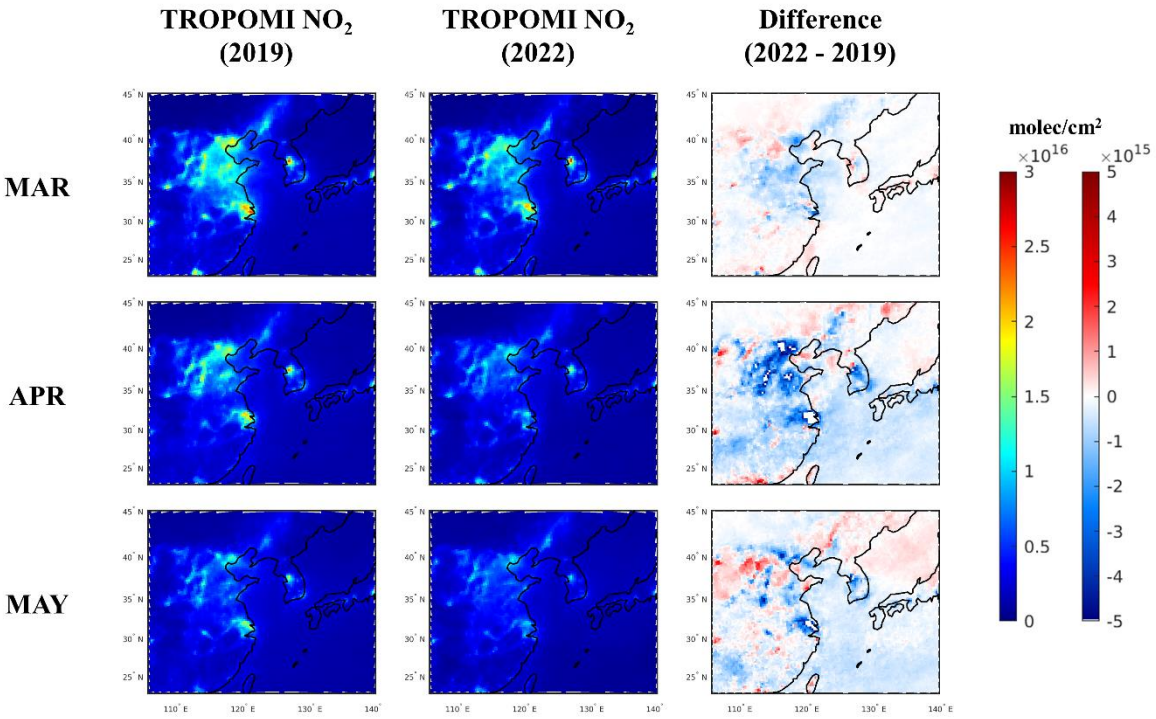

75 **Figure S9. Spatial distributions of TROPOMI NO_2 columns (molec/cm^2) in March, April, and May 2019 and 2022.**

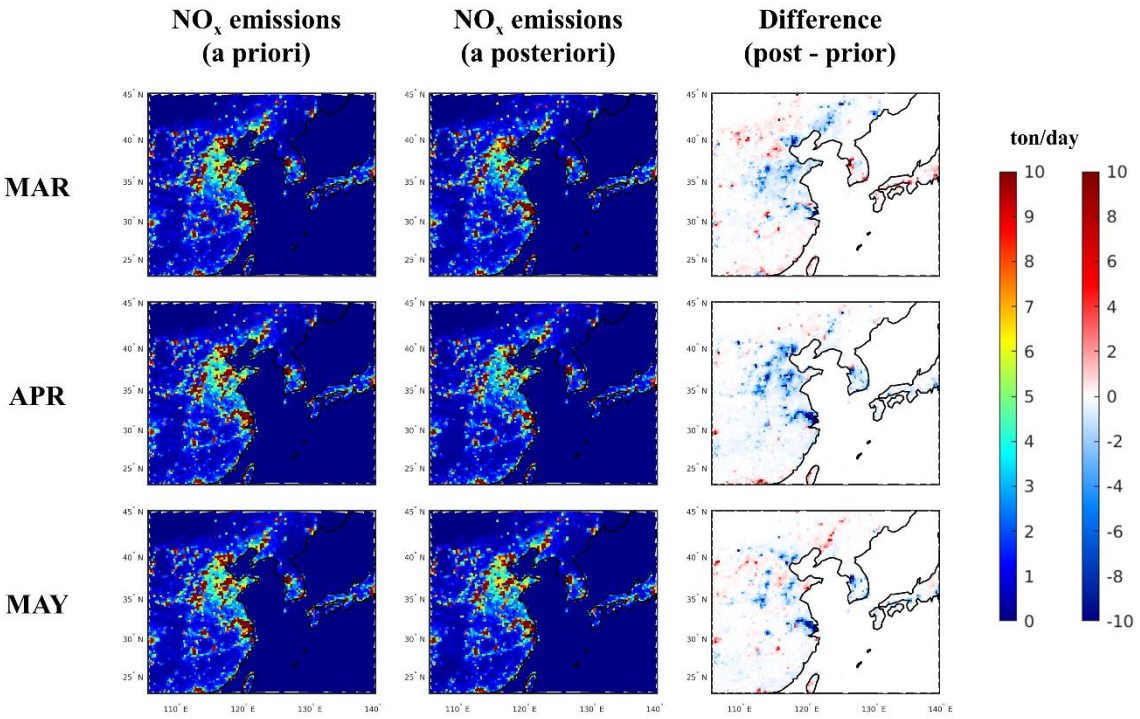

Figure S10. Spatial distributions of the bottom-up estimates of NO_x emissions (ton/day) before (a priori) and after (a posteriori) the NO_x emissions adjustment during the study period 2022.

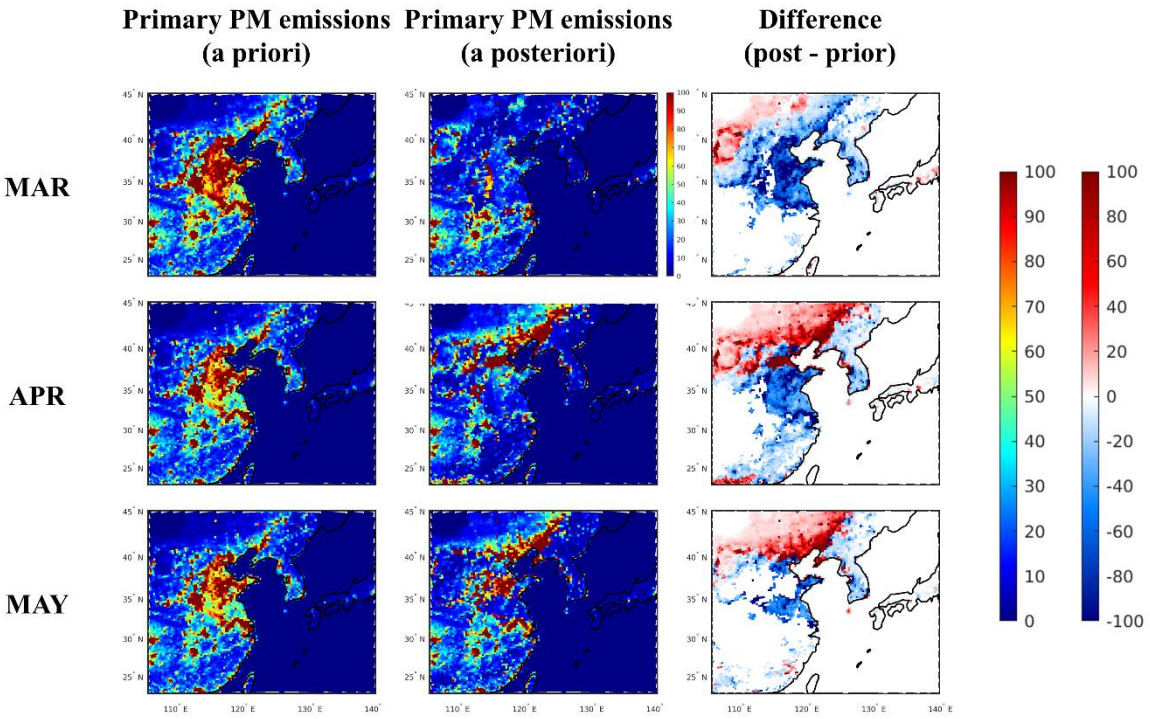

Figure S11. Spatial distributions of the bottom-up estimates of primary PM emissions (g/s) before (a priori) and after (a posteriori) the primary PM emissions adjustment (using GEMS-AMI-GOCI-2 fused AOD) during the study period 2022. The primary PM emissions here indicate the total amount of all primary PM species listed in Table S2.

References

Carter, W. P. L.: Development of the SAPRC-07 chemical mechanism. Atmos. Environ., 44(40), 5324–5335, https://doi.org/10.1016/j.atmosenv.2010.01.026, 2010.

Clough, S. A., Shephard, M. W., Mlawer, J. E., Delamere, J. S., Iacono, M. J., Cady-Pereira, K., et al.: Atmospheric radiative transfer modeling: A summary of the AER codes. J. Quant. Spectrosc. Ra., 91(2), 233–244, https://doi.org/10.1016/j.jqsrt.2004.05.058, 2005.

Iacono, M. J., Delamere, J. S., Mlawer, E. J., Shephard, M. W., Clough, S. A., and Collins, W. D.: Radiative forcing by long-lived greenhouse gases: Calculations with the AER radiative transfer models. J. Geophys. Res., 113, D13103, https://doi.org/10.1029/2008JD009944, 2008.

Jeon, W., Choi, Y., Lee, H. W., Lee, S.-H., Yoo, J.-W., Park, J., and Lee, H.-J.: A quantitative analysis of grid nudging effect on each process of $PM_{2.5}$ production in the Korean Peninsula. Atmos. Environ., 122, 763–774, https://doi.org/10.1016/j.atmosenv.2015.10.050, 2015.

Kain, J. S.: The Kain–Fritsch Convective Parameterization: An Update. J. Appl. Meteorol. Clim., 43(1), 170–181, https://doi.org/10.1175/1520-0450(2004)043<0170:TKCPAU>2.0.CO;2, 2004.

Morrison, H., Thompson, G., and Tatarskii, V. Impact of cloud microphysics on the development of trailing stratiform precipitation in a simulated squall line: Comparison of one- and two-moment schemes. Mon. Weather. Rev., 137(3), 991–1007, https://doi.org/10.1175/2008MWR2556.1, 2009.

Pleim, J. E., Xiu, A., Finkelstein, P. L., and Otte, T. L.: A Coupled Land-Surface and Dry Deposition Model and Comparison to Field Measurements of Surface Heat, Moisture, and Ozone Fluxes. Water, Air and Soil Pollution: Focus, 1(5), 243–252, https://doi.org/10.1023/A:1013123725860, 2001.

Pleim, J. E.: A Simple, Efficient Solution of Flux–Profile Relationships in the Atmospheric Surface Layer. J. Appl. Meteorol. Clim., 45(2), 341–347, https://doi.org/10.1175/JAM2339.1, 2006.

Pleim, J. E.: A Combined Local and Nonlocal Closure Model for the Atmospheric Boundary Layer. Part I: Model Description and Testing. J. Appl. Meteorol. Clim., 46(9), 1383–1395, https://doi.org/10.1175/JAM2539.1, 2007a.

Pleim, J. E.: A Combined Local and Nonlocal Closure Model for the Atmospheric Boundary Layer. Part II: Application and Evaluation in a Mesoscale Meteorological Model. J. Appl. Meteorol. Clim., 46(9), 1396–1409, https://doi.org/10.1175/JAM2534.1, 2007b.

Simon, H.: CMAQv5.0 PMother speciation. Community Multiscale Air Quality (CMAQ) Model Wiki, https://www.airqualitymodeling.org/index.php/CMAQv5.0_PMother_speciation (Accessed 15 July 2022), 2015.

Xiu, A., and Pleim, J. E.: Development of a Land Surface Model. Part I: Application in a Mesoscale Meteorological Model. J. Appl. Meteorol. Clim., 40(2), 192–209, https://doi.org/10.1175/1520-0450(2001)040<0192:DOALSM>2.0.CO;2, 2001.